ระเบียบวิธี Roe-FDS ที่มีเสถียรภาพสำหรับแก้ปัญหาการไร้เสถียรภาพของคลื่นช็อกบนตาข่ายสามเหลี่ยม

สุทธิศักดิ์ พงศ์ธนาพาณิช *

บทคัดย่อ

บทความนี้ได้ทำการศึกษาความไร้เสถียรภาพของระเบียบวิธีการแบ่งแยกฟลักซ์ของโรว์บนตาข่ายสามเหลี่ยม ในบางครั้งระเบียบวิธีนี้อาจนำมาสู่ผลลัพธ์ของการไร้ที่ไม่ถูกต้องตามหลักฟิสิกส์สำหรับปัญหาเฉพาะบางประเภท ปัญหาเหล่านี้รวมถึงปรากฏการณ์ปุ่มนูน หมายถึง โค้งที่ไม่สมจริงบนเส้นช็อกโค้งบริเวณใกล้แนวศูนย์กลางด้านหน้าของวัตถุโค้งมน หรือการเกิดการถูกรบกวนที่ไม่สมจริง เนื่องจากการเคลื่อนที่ของช็อกบทกริดที่มีการสูง-ต่ำแบบสลับฟันปลาในท่อตรง แนวคิดใหม่ของการแก้ไขค่าเอนโทรปีสำหรับตาข่ายสามเหลี่ยมแบบไร้ระเบียบได้ถูกนำเสนอเพื่อยกระดับการคำนวณหาผลลัพธ์ของคลื่นช็อก ระเบียบวิธีที่ถูกนำเสนอได้ถูกขยายผลสู่ความแม่นยำของผลลัพธ์ทั้งในพื้นที่และเวลาในลำดับสูงกว่า ความแม่นยำของผลลัพธ์ได้ถูกยกระดับขึ้นไปอีกด้วยการผนวกกระบวนการประมาณค่าความผิดพลาดเข้ากับอัลกอริทึมการปรับตาข่ายแบบอัตโนมัติ ประสิทธิภาพของกระบวนการที่ถูกผนวกเข้าด้วยกันได้ถูกประเมินโดยการวิเคราะห์พฤติกรรมช็อกเร็วเหนือเสียงและการแพร่กระจายของช็อกของการไหลแบบอัดตัวได้ความเร็วสูงทั้งในสภาวะคงตัวและไม่คงตัว

คำสำคัญ : ระเบียบวิธีการแบ่งแยกฟลักซ์ของโรว์, แก้ไขค่าเอนโทรปี, คลื่นช็อก

ภาควิชาเทคโนโลยีวิศวกรรมเครื่องกล วิทยาลัยเทคโนโลยีอุตสาหกรรม มหาวิทยาลัยเทคโนโลยีพระจอมเกล้าพระนครเหนือ กรุงเทพฯ 10800,
* ผู้ติดต่อ, อีเมล์ : sutthisakp@kmutnb.ac.th รับเมื่อ 28 กุมภาพันธ์ 2556 ตอบรับเมื่อ 24 เมษายน 2556

Stabilized Roe-FDS Scheme for Solving Shock Wave Instabilities Problems on Triangular Grids

Sutthisak Phongthanapanich*

Abstract

This paper study the numerical instability of Roe's flux-difference splitting scheme on triangular grids. The scheme may sometimes lead to unphysical flow solutions in certain problems. These problems include the carbuncle phenomenon that refers to a spurious bump on the bow shock near the flow center line ahead the blunt body or an unrealistic perturbation that occurs from a moving shock along odd-even grid perturbation in a straight duct. The new idea of entropy fix for unstructured triangular grids is presented to improve the computed shock wave resolution. The proposed scheme is further extended to obtain higher-order spatial and temporal solution accuracy. The solution accuracy is further improved by coupling an error estimation procedure to an adaptive remeshing algorithm. Efficiency of the combined procedure is evaluated by analyzing supersonic shocks and shock propagation behaviors for both the steady and unsteady high-speed compressible flows.

Keywords : Roe's flux-difference splitting scheme, entropy fix, shock wave

---

Mechanical Engineering Technology Department, College of Industrial Technology, King Mongkut's University of Technology North Bangkok,

* Corresponding author, E-mail : sutthisakp@kmutnb.ac.th Received 28 February 2013, Accepted 24 April 2013

1. Introduction

High-speed compressible flows normally involve complex flow phenomena, such as strong shock waves, shock-shock interactions and shear layers. Numerical flux formulation is an essential part of flux formulation schemes in order to obtain accurate and robustness numerical solutions of the Euler equations. Various numerical inviscid flux formulations have been proposed to solve an approximate Riemann problem. Among these formulations, the flux-difference splitting scheme by Roe [1] is widely used due to its accuracy, quality and mathematical clarity. However, the scheme may sometimes lead to unphysical flow solutions in certain problems. These problems include the carbuncle phenomenon that refers to a spurious bump on the bow shock near the flow center line ahead the blunt body; an unrealistic perturbation [2] that occurs from a moving shock along odd-even grid perturbation in a straight duct; and a kinked Mach stem observed when a normal shock wave reflects on a ramp to form a double-Mach reflection.

The main objectives of this paper are to propose and evaluate a stabilized Roe-FDS scheme with adaptive unstructured grids for two-dimensional high-speed compressible flow analysis. The *H*-correction entropy fix [3,4] is modified for unstructured triangular grids and implemented into the original Roe's scheme. To improve the analysis solution accuracy, the presented scheme is further extended to high-order solution accuracy and combined with an adaptive grid procedure. To enhance solution accuracy of the numerical analysis, the grid adaptation is needed to improve the computed solution. An adaptive grid technique is incorporated with an appropriated error indicator to dictate a close correlation between the size of cells and the behavior of the corresponding computed solution. The technique is implemented to capture fast variation of the solution with a reasonable number of elements. The process of the adaptive grid is to first generate initial grid of the domain. The grid is used to compute the corresponding solution by the finite volume method. Then the regions where adaptation is vital are determined by an error indicator. A new grid, which is better adapted for the solution, is entirely created. The same process is repeated until the specified convergence criterion is met. The efficiency of the overall procedure is evaluated using examples in the field of computational fluid dynamics that include the supersonic shock waves and shock propagation behaviors. The efficiency of the combined procedure is evaluated by analyzing a series of both steady and unsteady high-speed compressible flows.

2. Stabilized Roe's Flux-Difference Splitting Scheme

The finite volume formulation of two-dimensional Euler equations for high-speed compressible flows of an element with domain Ω may be written in the form,

$$\frac{\partial}{\partial t}\int_{\Omega}\vec{U}\,d\Omega+\oint_{\partial\Omega}\vec{F}\cdot\vec{n}dS=0 \qquad (1)$$

where Ω is a control volume. $\vec{U}$ is the vector of conservative variables, and $\vec{F}$ is the vector of the convective fluxes. The Roe's approximate Riemann solver (**Roe**) is implemented in the framework of the cell-centered scheme. The numerical flux, passing through a shared side of the two adjacent left and right elements is given by [1],

$$\boldsymbol{F}_n = \frac{1}{2}(\boldsymbol{F}_{nL} + \boldsymbol{F}_{nR}) - \frac{1}{2}\sum_{k=1}^{4}\alpha_k|\lambda_k|\boldsymbol{r}_k \qquad (2)$$

where α_k is the wave strength of the k^{th} wave, λ_k is the eigenvalue $\lfloor V_n - a \quad V_n \quad V_n \quad V_n + a \rfloor^T$, $\boldsymbol{r}_k$ is the corresponding right eigenvector, V_n is the normal velocity, and a is the speed of sound at the cell interface.

Sanders *et al.* [3] introduced an idea of a multidimensional dissipation, the so called *H*-correction entropy fix method. This method is then modified for unstructured triangular grid as shown by Fig. 1(a) and it has shown to eliminate the unrealistic carbuncle phenomenon of the flow over a blunt body in the structured uniform grid [4]. The advantages of the method are the simplicity in the implementation into the existing scheme and the parameter-free characteristics. For the two triangular cells shown in Fig. 1(b), the stabilized eigenvalues have been proposed by,

$$\eta^{SP} = \max(\eta_2, \eta_3, \eta_4, \eta_5) \qquad (3)$$

where η_i, i = 2 to 5 are,

$$\eta_i = 0.5\max_k(|\lambda_{kR} - \lambda_{kL}|) \qquad (4)$$

Then the eigenvalues are modified according to Harten [5] yielding,

$$\lambda_k^{SP} = \max\left(\lambda_k, \eta^{SP}\right) \qquad (5)$$

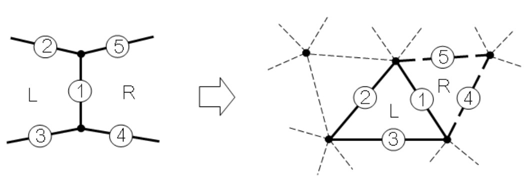

(a) (b)

Fig. 1. Control volume topology of (a) structured uniform grid, and (b) unstructured triangular grid.

It has been found that the above method performs well on certain problems but may fail for the others. Thus, this paper proposes a stabilized Roe-FDS method (**RoeSP**) that combines the entropy fix method of Van Leer *et al*. [6] and the modified multidimensional dissipation method by Pandolfi and D'Ambrosio [7], the modified *H*-correction, together by replacing the original eigenvalues as follows,

$$|\lambda_k| = \begin{cases} |\lambda_{1,4}| & , |\lambda_{1,4}| \geq 2\eta^{VL} \\ \dfrac{|\lambda_{1,4}|^2}{4\eta^{VL}} + \eta^{VL} & , |\lambda_{1,4}| < 2\eta^{VL} \\ \max\left(|\lambda_{2,3}|, \eta^{SP}\right) & \end{cases} \qquad (6)$$

where $\eta^{VL} = \max\left(\lambda_R - \lambda_L, 0\right)$.

To illustrate an unphysical expansion shock, a Mach 6 moving shock along odd-even grid perturbation in a straight duct [2]. The computational domain consists of a uniform triangular grid with 800 and 20 equal intervals respectively along the axial and the transverse directions of the duct. The grids along the duct centerline are perturbed in the transverse direction with magnitude of $\pm 10^{-6}$. The **RoeSP** can provide accurate shock resolution whereas the **Roe** suffers from the numerical instabilities as depicted in figures 2(a)-(h), respectively. As explained by Gressier and Moschetta [8], the exact capture of contact discontinuity and strict stability cannot be simultaneously satisfied in any upwind scheme. The solution suggests that additional dissipation injection to the entropy and shear waves is thus needed to stabilize the Roe's scheme as done by **RoeSP**.

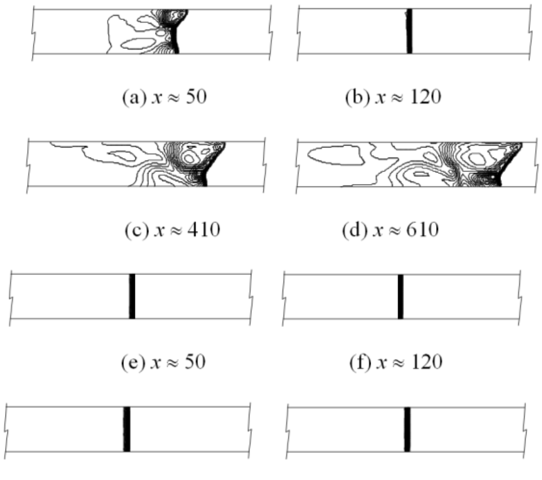

Fig. 2. Density contours of a Mach 6 moving shock along odd-even grid perturbation problem: (a)-(d) **Roe**; and (e)-(h) **RoeSP**.

The second unrealistic flow solution, the so-called carbuncle phenomenon, of a steady-state flow over a blunt body from the original Roe's scheme was first reported by Perry and Imlay [9]. Such phenomenon refers to a spurious bump on the bow shock near the flow center line ahead the blunt body. The phenomenon is highly grid-dependent [7] but does not require a large number of grid points to appear [8]. To demonstrate this grid-dependent phenomenon, the methods are employed with three meshes of different element aspect ratios. An enlarged view of the elements near the flow centerline of the grid and the corresponding density contours are shown in Figs. 3(a)-(c). The carbuncle phenomenon can be clearly seen in a more refined grid with higher element aspect ratio as shown in Fig. 3(a). While the **RoeSP** provides reasonable flow solutions, the carbuncle phenomena are easily observed in the Fig. 3(c).

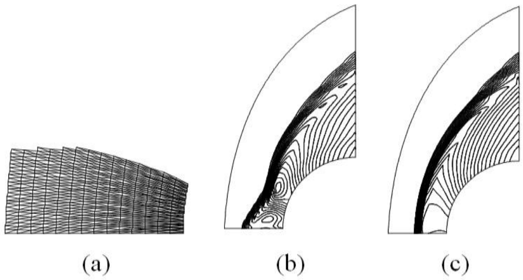

Fig. 3. Mach 15 flow over a blunt body problem: (a) enlarged view of the mesh; (b) **Roe**; and (c) **RoeSP**.

3. Higher-Order Formulation

Solution accuracy from the first-order formulation described in the preceding sections can be improved by implementing a high-order formulation for both the space and time. A high-order spatial discretization is achieved by applying the Taylor' series expansion to the cell-centered solution for each cell face [10]. For instance, the solutions at the midpoint of an element edge between node 1 and 2, can be reconstructed from,

$$\boldsymbol{q}_{f_{1-2}} = \boldsymbol{q}_C + \frac{\Psi_C}{3}\left[\frac{(\boldsymbol{q}_1 + \boldsymbol{q}_2)}{2} - \boldsymbol{q}_3\right] \quad (7)$$

where $\boldsymbol{q} = [\rho \quad u \quad v \quad p]^T$ consists the primitive variables of the density, the velocity components, and the pressure, respectively; $\boldsymbol{q}_C$ is the solution at the element centroid; $\boldsymbol{q}_n$, n = 1, 2, 3 are the solutions at nodes. In this paper, the inverse-distance weighting from the centroid to the nodes that preserves the principle of positivity is used,

$$\boldsymbol{q}_n = \sum_{i=1}^{N} \frac{\boldsymbol{q}_{C,i}}{|\vec{\boldsymbol{r}}_i|} \Bigg/ \sum_{i=1}^{N} \frac{1}{|\vec{\boldsymbol{r}}_i|} \quad (8)$$

where $\boldsymbol{q}_{C,i}$ are the surrounding cell-centered values of node n. $|\vec{\boldsymbol{r}}_i|$ is the distance from the centroid to node n, and N is the number of the surrounding cells.

The Ψ_C in Eq. (7) represents the limiter, preventing spurious oscillation that may occur in the region of high gradients. In this study, Vekatakrishnan's limiter function [11] is selected,

$$\Psi_C = \min_{i=1,2,3} \begin{cases} \phi\left(\dfrac{\Delta_{+,\max}}{\Delta_-}\right) & , \Delta_- \geq 0 \\ \phi\left(\dfrac{\Delta_{+,\min}}{\Delta_-}\right) & , \Delta_- < 0 \\ 1 & , \Delta_- = 0 \end{cases} \tag{9}$$

where $\Delta_- = \boldsymbol{q}_c - \boldsymbol{q}_i$, $\Delta_{+,\max} = \boldsymbol{q}_{\max} - \boldsymbol{q}_i$, and $\Delta_{+,\min} = \boldsymbol{q}_{\min} - \boldsymbol{q}_i$. The $\boldsymbol{q}_{\max}$ and $\boldsymbol{q}_{\min}$ are respectively the maximum and minimum values of all distance-one neighboring cells. The function ϕ is similar to the Van Albada limiter [12], which is expressed in the form,

$$\phi(y) = \frac{y^2 + 2y}{y^2 + y + 2} \tag{10}$$

The second-order temporal accuracy is achieved by implementing the second-order accurate Runge-Kutta time stepping method [13],

$$\begin{aligned} \boldsymbol{U}_i^* &= \boldsymbol{U}_i^n - \frac{\Delta t}{\Omega_i} \sum_{j=1}^{3} \boldsymbol{F}^n \cdot \boldsymbol{n}_j \\ \boldsymbol{U}_i^{n+1} &= \frac{1}{2}\left[\boldsymbol{U}_i^0 + \boldsymbol{U}_i^* - \frac{\Delta t}{\Omega_i} \sum_{j=1}^{3} \boldsymbol{F}^* \cdot \boldsymbol{n}_j\right] \end{aligned} \tag{11}$$

where Δt is the time step.

The high-order extension of the **RoePA** presented in the preceding section is evaluated by solving several problems. The modified scheme is also combined with an adaptive grid technique that generates unstructured triangular grids for more complex problems. These selected test cases are: (1) Sod shock tube, (2) Supersonic flow over a bump, and (3) Steady-state Mach 15.3 flow past a cylinder.

4. Results and Discussions

4.1 Sod Shock Tube

The one-dimensional shock tube test case, the so called Sod shock tube [14], is solved by using a two-dimensional domain. The initial conditions of the fluids on the left and right sides are given by $(\rho, i, p)_L = (1.0, 0.0, 1.0)$ and $(\rho, i, p)_R = (0.125, 0.0, 0.1)$. The 1.0 × 0.1 computational domain is discretized with uniform triangular elements into 400 and 40 equal intervals in the *x* and *y* directions, respectively. Figures 4(a)-(b) show the predicted density and pressure both first and second-order accurate distributions along the tube length and are compared with the exact solutions at time *t* = 0.15. The figures show that the second-order extension of **RoeSP** provides more accurate solutions than the first-order solutions.

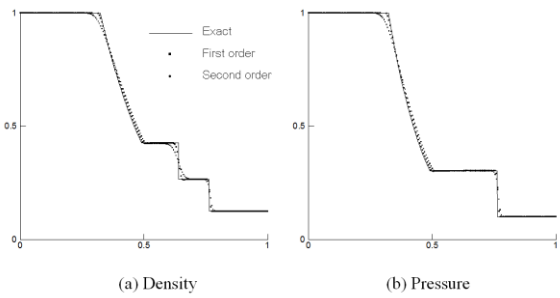

Fig. 4. Comparison of numerical and exact solutions at time *t* = 0.15.

4.2 Supersonic flow over a bump

The second-order **RoeSP** is further evaluated for adaptive unstructured grids using a problem with more complex flow phenomena. Figure 5 shows the problem statement of a supersonic flow over a 4% bump with a Mach 1.4 flows from the left side of domain which results in complex flow behavior. The initial grid and the corresponding density contours computed by using the second-order **RoeSP** are shown in Figs. 6(a)-(b), respectively. The adaptive technique [15-17] is then used to capture solution discontinuities in order to enhance the solution accuracy. The final adaptive grid and the corresponding density contours computed by using the second-order **RoeSP** are shown in Figs. 6(c)-(d), respectively. The figures highlight the use of the second-order accurate scheme on adaptive grids to effectively obtain detailed flow solution.

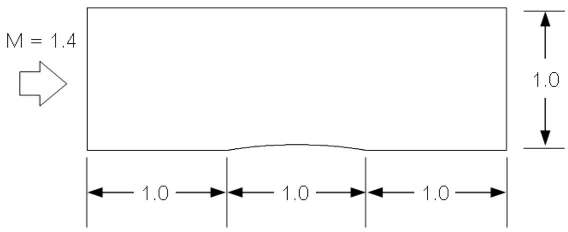

Fig. 5. Problem statement of a supersonic flow over a bump.

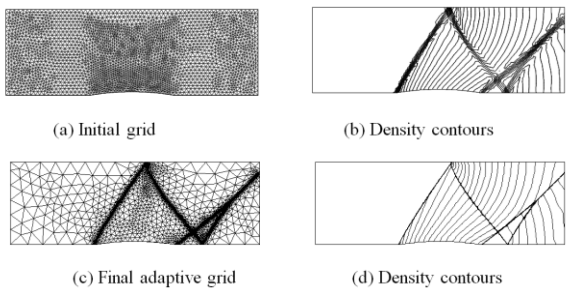

Fig. 6. A supersonic flow over a bump problem.

4.3 Steady-state Mach 15.3 flow past a cylinder

The last problem that used to demonstrate the solution accuracy improvement by coupling a **RoeSP** to a remeshing algorithm is a steady-state Mach 15.3 flow past a cylinder is described in Fig. 7. Figures 8(a)-(d) show the adaptive grid consisting of 36,986 cells, as well as the resulting density, pressure and Mach number contours. The figures show that the second-order extension of **RoeSP** provides more accurate solutions without spurious bump ahead of a blunt body.

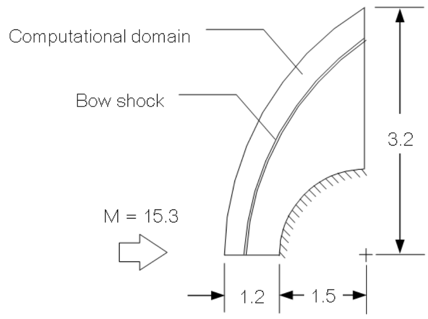

Fig. 7. A supersonic flow over a bump problem.

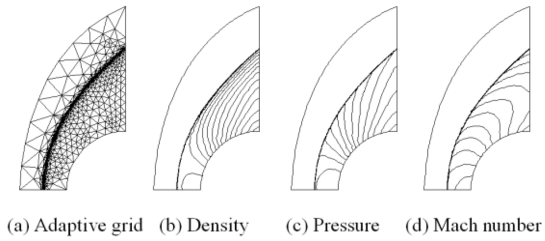

Fig. 8. A supersonic flow over a bump problem.

5. Conclusions

The modified *H*-correction entropy fix (**RoeSP**) for unstructured triangular grids is proposed to improve numerical stability of the Roe's flux-difference splitting scheme. The method was then evaluated by several well-known test cases and found to eliminate unphysical solutions that may arise from the use of the original Roe's scheme. These unphysical solutions include the expansion shock generated from the flow over a forward facing step and numerical instability from the odd-even decoupling problem. To further improve solution accuracy, the second-order spatial and second-order Runge-Kutta temporal discretization were also implemented. The method was also combined with an adaptive grid generation technique to demonstrate its applicability for arbitrary unstructured grids. The entire process was found to provide more accurate solutions for both the steady-state and transient flow test cases.

6. Acknowledgements

The authors are pleased to acknowledge the College of Industrial Technology, King Mongkut's University of Technology North Bangkok (KMUTNB), and the National Metal and Materials Technology Center (MTEC) for supporting this research work.

7. References

[1] P.L. Roe, "Approximate Riemann Solvers, Parameter Vectors, and Difference Schemes", Journal of Computational Physics, 43, 1981, pp. 357-372.

[2] J.J. Quirk, "A Contribution to the Great Riemann Solver Debate", International Journal for Numerical Methods in Fluids, 18, 1994, pp. 555-574.

[3] R. Sanders, E. Morano and M.C. Druguet, "Multidimensional Dissipation for Upwind Schemes: Stability and Applications to Gas Dynamics", Journal of Computational Physics, 145, 1998, pp. 511-537.

[4] P. Dechaumphai and S. Phongthanapanich, "High-Speed Compressible Flow Solutions by Adaptive Cell-Centered Upwinding Algorithm with Modified *H*-Correction Entropy Fix", Advances in Engineering Software, 34, 2003, pp. 533-538.

[5] A. Harten, "High Resolution Schemes for Hyperbolic Conservation Laws", Journal of Computational Physics, 49, 1983, pp. 357-393.

[6] B. Van Leer, W.T. Lee and K.G. Powell, "Sonic-Point Capturing", AIAA Paper-89-1945-CP, AIAA, 9th Computational Fluid Dynamics Conference, New York, 1989.

[7] M. Pandolfi and D. D'Ambrosio, "Numerical Instabilities in Upwind Methods: Analysis and Cures for the "Carbuncle" Phenomenon", Journal of Computational Physics, 166, 2001, pp. 271-301.

[8] J. Gressier and J.M. Moschetta, "Robustness versus Accuracy in Shock-wave Computations", International Journal for Numerical Methods in Fluids, 33, 2000, pp. 313-332.

[9] K.M. Perry and S.T. Imlay, "Blunt-Body Flow Simulations," AIAA Paper-88-2904, 24th AIAA, SAE, ASME and ASEE Joint Propulsion Conference, MA, 1988.

[10] S. Phongthanapanich and P. Dechaumphai, "Flux-Difference Splitting Scheme with Modified Multidimensional Dissipation on Unstructured Meshes", Journal of the Chinese Institute of Engineers, 27, 2004, pp. 981-992.

[11] V. Vekatakrishnan, "Convergence to Steady State Solutions of the Euler Equations on Unstructured Grids with Limiters", Journal of Computational Physics, 118, 1995, pp. 120-130.

[12] G.D. Van Albada, B. Van Leer and W.W. Roberts, "A Comparative Study of Computational Methods in Cosmic Gas Dynamics", Astronomy and Astrophysics, 108, 1982, pp. 76-84.

[13] C.W. Shu and S. Osher, "Efficient Implementation of Essentially Non-oscillatory Shock-capturing Schemes", Journal of Computational Physics, 77, 1988, pp. 439-471.

[14] G.A. Sod, "A Survey of Several Finite Difference Methods for Systems of Nonlinear Hyperbolic Conservation Laws", Journal of Computational Physics, 27, 1978, pp. 1-31.

[15] S. Phongthanapanich and P. Dechaumphai, "Adaptive Finite Element Method for Crack Propagation Analysis", The Journal of King Mongkut's University of Technology North Bangkok, 19, 2009 , pp. 154-163.

[16] S. Phongthanapanich, "An Explicit Finite Volume Element Method without an Explicit Artificial Diffusion Term for Convection-Diffusion Equation on Triangular Grids", Thammasart International Journal of Science & Technology, 15, 2010, pp. 69-80.

[17] S. Phongthanapanic, "Triangular Mesh Generation for Finite Element/Finite Volume Methods", The Journal of Industrial Technology, 8, 2012, pp. 9-18.